

# UNIVERSIDAD DE CONCEPCIÓN



## CENTRO DE INVESTIGACIÓN EN INGENIERÍA MATEMÁTICA (CI<sup>2</sup>MA)



**First insights into the performance of the SWOT Level 2 River  
Single-Pass Vector Data Product in rivers with complex  
morphology: application to the Bío-Bío River basin, Chile**

RODRIGO ABARCA DEL RIO, FERNANDO CAMPOS,  
CRISTÓBAL CARO-RAMÍREZ, JEAN FRANÇOIS CRETAUX,  
DANIEL MOREIRA, ALFREDO RIBEIRO NETO,  
JONAS FELIPE SANTOS DE SOUZA, MAURICIO SEPÚLVEDA

PREPRINT 2026-05

SERIE DE PRE-PUBLICACIONES



1 Authors: Cristóbal Caro-Ramírez<sup>1</sup>, Rodrigo Abarca-Del-Río<sup>2</sup>, Mauricio Sepúlveda<sup>3</sup>, Fernando Campos<sup>4</sup>,  
2 Alfredo Ribeiro Neto<sup>5</sup>, Jonas Felipe Santos de Souza<sup>6</sup>, Jean François Cretaux<sup>7</sup>, Daniel Moreira<sup>8</sup>.

3 “First insights into the performance of the SWOT Level 2 River Single-Pass Vector Data Product in rivers  
4 with complex morphology: application to the Biobío River basin, Chile.”

## 5 Abstract

6 Hydrological monitoring in Chile is hindered by sparse and unevenly distributed gauging networks,  
7 particularly in mountain basins with limited accessibility. The Surface Water and Ocean Topography  
8 (SWOT) mission offers a unique opportunity to complement *in situ* observations through high-resolution  
9 radar altimetry. The Biobío River basin presents a demanding environment for SWOT due to its narrow  
10 channels, steep gradients, and strong geomorphological heterogeneity.

11 This study evaluates the performance of the SWOT L2\_HR\_RiverSP (version C) product in the Biobío  
12 basin by comparing satellite-derived water-surface elevations with *in situ* measurements from nine DGA  
13 streamflow stations. Standard hydrological metrics (R, NSE, NRMSE, MAE) were applied along with  
14 quality filters ( $wse\_u < 0.15$ ;  $node\_q = 0-1$ ). Results show strong spatial variability linked to channel  
15 width and morphology: wide reaches ( $>200$  m) exhibit high correlations ( $R \approx 0.80$ ) and moderate errors  
16 ( $NRMSE < 0.7$ ), whereas narrow or sinuous segments yielded negative NSE values and substantial  
17 dispersion. Geometric inconsistencies in the SWORD database were also identified, along with  
18 indications of reduced observational consistency following the transition to version D, although this  
19 version was not formally analyzed.

20 Overall, SWOT shows considerable potential for enhancing hydrological observation in Chile, but its  
21 operational application in narrow or morphologically complex rivers requires local validation, geometric  
22 correction, and integration with lower-level products (e.g., PIXC) to better interpret observations under  
23 challenging fluvial conditions.

24 Keywords: SWOT, satellite altimetry, river hydrology, validation, Biobío River, SWORD.”

25  
26  
27  
28  
29  
30

1. Universidad de Concepción, Facultad de Ciencias Ambientales, Víctor Lamas 1290, Concepción, Chile – [crisob.car@gmail.com](mailto:crisob.car@gmail.com)
2. Universidad de Concepción, Facultad de Ciencias Físicas y Matemáticas, Víctor Lamas 1290, Concepción, Chile-  
[rabarca@rio.univ@gmail.com](mailto:rabarca@rio.univ@gmail.com)
3. CI2MA and Departamento de Ingeniería Matemática, Facultad de Ciencias Físicas y Matemáticas, Universidad de Concepción,  
Concepción, Chile – [maursepu@udec.cl](mailto:maursepu@udec.cl)
4. CI2MA and Departamento de Ingeniería Matemática, Facultad de Ciencias Físicas y Matemáticas, Universidad de Concepción,  
Concepción, Chile – [fcamposg@udec.cl](mailto:fcamposg@udec.cl)
5. Departamento de Engenharia Civil e Ambiental, Universidade Federal de Pernambuco, Rua Acadêmico Hélio Ramos - Cidade  
Universitária, Recife - PE, 50740-467 - [alfredo.ribeiro@ufpe.br](mailto:alfredo.ribeiro@ufpe.br)
6. Departamento de Engenharia Civil e Ambiental, Universidade Federal de Pernambuco, Rua Acadêmico Hélio Ramos - Cidade  
Universitária, Recife - PE, 50740-467 - [jonas.ssouza@ufpe.br](mailto:jonas.ssouza@ufpe.br)
7. Laboratoire d'Études en Géophysique et Océanographie Spatiales (LEGOS), CNES-IRD-CNRS-UT3, Université de Toulouse, Toulouse,  
France - [Jean-francois.cretaux@legos.obs-mip.fr](mailto:Jean-francois.cretaux@legos.obs-mip.fr)
8. Geological Survey of Brazil, Rio de Janeiro, Brazil and Geosciences Environnement Toulouse (GET), Université Toulouse,IRD, CNRS,  
CNES, UT, Toulouse, France - [daniel.moreira@sgb.gov.br](mailto:daniel.moreira@sgb.gov.br)

31

## 32 **1. Introduction**

33 Rivers play essential ecological, social, and economic roles worldwide, shaping landscapes, supporting  
34 biodiversity, and providing critical ecosystem services such as water supply, climate regulation, and  
35 aquifer recharge (Zeiringer, Seliger, Greimel, & Schmutz, 2018). In Chile, these functions acquire  
36 particular relevance given the country's dependence on rivers for hydropower generation, irrigation,  
37 and urban water supply, especially in regions affected by high climatic variability and increasing pressure  
38 on water resources (OECD, 2024). However, river systems are among the most threatened globally due  
39 to anthropogenic interventions, hydropower development, land-use change, and the accelerating  
40 impacts of climate change, all of which modify natural flow regimes and reduce the predictability of  
41 extreme hydrological events (Malmqvist and Rundle, 2002; Poff et al., 1997). In Chile, these pressures  
42 have intensified hydromorphological alteration in multiple basins (Rojas et al., 2019; Rojas et al., 2014),  
43 amplifying the need for robust and spatially extensive hydrological monitoring systems.

44 Despite this need, traditional hydrological observation in Chile faces severe limitations. The national  
45 gauging network exhibits low spatial density, irregular maintenance, gaps in temporal continuity, and  
46 insufficient coverage in mountain and remote regions (Mesa Nacional del Agua, 2022; Nicolás Vásquez  
47 et al., 2021). These deficiencies hinder the construction of reliable hydrological reference series, the  
48 calibration of hydrological models, and the development of adaptive water-management strategies  
49 under changing climatic conditions (Fustos et al., 2022; Muñoz et al., 2011; Wade et al., 2025). As  
50 recognized in global and Chilean contexts, data scarcity in ungauged or poorly gauged basins remains a  
51 major challenge for hydrological research and water-resources planning (Hrachowitz et al., 2013).

52 The Surface Water and Ocean Topography (SWOT) satellite mission represents a significant  
53 advancement in the remote observation of continental waters by providing high-resolution  
54 measurements of water surface elevation, width, and slope using Ka-band interferometric radar  
55 (Biancamaria et al., 2016). For rivers wider than 50 m, SWOT can achieve vertical accuracies of  
56 approximately 10 cm, offering new opportunities for monitoring hydrological variability, calibrating  
57 discharge models, and assessing surface-water dynamics (Moreira et al., 2025; Yao et al., 2025). These  
58 capabilities are particularly relevant for countries like Chile, where complex topography and accessibility  
59 constraints limit the expansion of conventional gauging networks.

60 However, important knowledge gaps remain regarding SWOT performance in fluvial environments  
61 characterized by narrow channels, steep longitudinal profiles, dense riparian vegetation, or high  
62 morphological variability. Such conditions are common in Chilean basins influenced by the Andes and  
63 the Coastal Range, where sinuosity, confined valleys, islands, and irregular planforms may affect radar  
64 detection and lead to systematic errors in water-surface retrievals. International studies have  
65 documented challenges in similar settings, showing that river width, geometric complexity, and  
66 vegetation can degrade SWOT observations (Andreadis et al., 2025; Andreoli et al., 2012; Zhao et al.,  
67 2025). These findings highlight the need for regional validation to determine the mission's reliability in  
68 morphologically complex basins and in rivers near or below the nominal width threshold.

69 The Biobío River basin provides an ideal testbed for this purpose. It is one of the largest and most  
70 hydrologically significant basins in Chile, spanning strong physiographic and climatic gradients from the  
71 Andes to the Pacific, and containing multiple tributaries with contrasting morphologies (DGA, 2012;

72 Figueroa et al., 2020). The basin also includes heavily regulated sections influenced by major  
73 hydroelectric infrastructure, which can further alter water-surface properties and affect radar  
74 backscatter. These conditions make the Biobío a particularly demanding environment for evaluating  
75 SWOT performance.

76 To date, no formal evaluation exists of SWOT river products in Chile, nor in Andean basins with narrow,  
77 steep, and geomorphologically heterogeneous channels. This represents a critical gap given the  
78 country's dependence on satellite-based observations to complement sparse *in situ* networks.

79 This study provides a regional validation of the SWOT L2\_HR\_RiverSP product (version C) in Chile by  
80 comparing satellite-derived water-surface elevations with *in situ* measurements from nine streamflow  
81 stations operated by the Dirección General de Aguas (DGA).

82 Although this is a first insight, this study aims to:

83 (1) Quantify the agreement between SWOT and *in situ* observations across a range of channel  
84 morphologies.

85 (2) Evaluate how width, sinuosity, and local geomorphology influence detection quality.

86 (3) Identify geometric discrepancies in the SWOT database and assess their impact on SWOT retrievals.

87 This study provides insights through evidence-based assessment of SWOT performance in Chile and  
88 offers a foundation for the mission's operational use in Andean basins with complex morphology and  
89 limited *in situ* observation.

## 90 **2. Study Area**

### 91 ***2.1 Physiographic characteristics of the Biobío River basin***

92 The Biobío River basin, one of the largest and most important in Chile, covers approximately 23,861 km<sup>2</sup>  
93 between 36°42' and 38°49' S and 71°00' and 73°20' W. Its main river originates in Galletué Lagoon  
94 (1,160 m a.s.l.) in the Andes Mountains and flows roughly 380 km before reaching its outlet in the Gulf  
95 of Arauco (Pacific Ocean). Among its principal tributaries are the Vergara, Laja, Duqueco, Queuco, and  
96 Bureo rivers, all of which contribute substantial discharge to the system (Figueroa, Parra, & Díaz, 2020).

97 From a morphostructural perspective, the basin is organized into three well-defined physiographic units:  
98 the Andes Mountains to the east, the Central Depression in the middle sector, and the Coastal Range to  
99 the west. This arrangement creates a marked altitudinal gradient that controls fluvial energy and  
100 conditions the dynamics of hydrological and sedimentary processes (DGA, 2012).

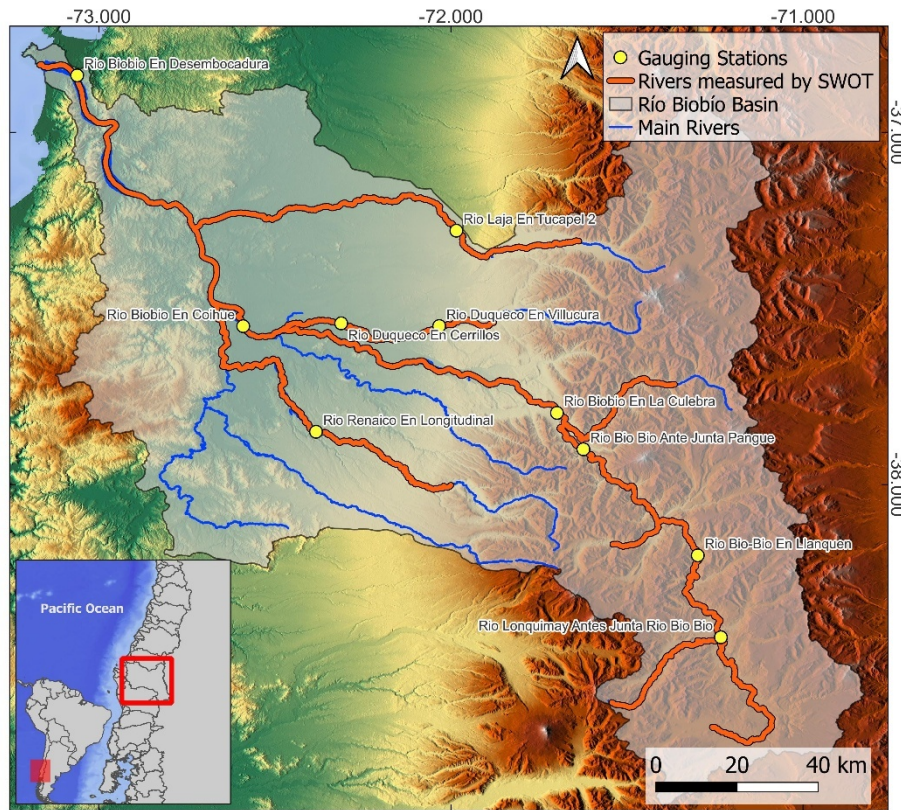


Figure 1. Study Area: Río Biobío Basin

101

102

103 **2.2 Morphology, climate, and hydrological regime**

104 The morphology of the basin varies markedly along its course. In the upper basin, narrow glacial valleys  
 105 with steep slopes predominate; in the middle section, the river crosses a fluviovolcanic plain associated  
 106 with the Antuco volcano; and in the lower reach, the Biobío flows over a fluvio-marine plain  
 107 characterized by recent deposits and high sedimentary dynamics.

108 Climatically, the basin exhibits a pronounced latitudinal and altitudinal gradient. Annual precipitation  
 109 ranges from about 1,000 mm in the central valley to more than 2,000 mm in the high Andes, with most  
 110 rainfall occurring during winter. This distribution generates a nivo-pluvial hydrological regime, with  
 111 winter and spring flow maxima driven by frontal rainfall and snowmelt (DGA, 2012; Figueroa et al.,  
 112 2020).

113 The Biobío River is one of the highest-discharge rivers in the country, with an average annual flow of  
 114 approximately 900 m<sup>3</sup>/s at its mouth. This behavior makes it a representative system for validating  
 115 satellite observations under conditions of strong topographic and climatic contrast.

116 **2.3. Anthropogenic pressure and hydroelectric infrastructure.**

117 The basin has been heavily modified by human activities, particularly through the construction of large-  
 118 scale hydroelectric power plants such as Ralco, Pangué, and Angostura, which significantly alter the  
 119 river's natural regime. These facilities regulate flow, reduce seasonal variability, and modify downstream  
 120 sedimentary and ecological dynamics (Figueroa et al., 2020).

121 Other sub-basins, such as those of the Laja and Duqueco rivers, also contain regulation systems and  
122 reservoirs that increase hydromorphological alteration. Combined with land-use change and projected  
123 flow reductions due to climate change, these pressures create a scenario of high hydrological  
124 vulnerability (DGA, 2012; Figueroa et al., 2020).

125 Taken together, these conditions make the Biobío River basin an ideal environment for assessing the  
126 accuracy and limitations of satellite products such as SWOT, particularly in rivers with complex  
127 morphologies and strong anthropogenic interference.

## 128 **2 Data and Methodology**

### 129 ***2.1. Satellite and geometric data (SWOT, SWORD, Sentinel-2)***

130 The analysis was based on the vector product of the SWOT mission, known as the Level-2 High Rate  
131 River Single-Pass Vector Data Product (L2\_HR\_RiverSP, version C). This dataset provides estimates of  
132 water surface elevation (WSE), its associated uncertainty (*wse\_u*), the node quality index (*node\_q*), and  
133 other hydrological attributes defined for river reaches and nodes included in the SWORD (SWOT River  
134 Database) framework (Altenau et al., 2025).

135 SWOT's satellite configuration enables near-global coverage, with high-resolution observations (~50–70  
136 m) acquired over 50-km swaths on each side of the orbit. For this study, all observations available from  
137 the beginning of version C records were used; the first acquisition cycles for rivers in Chile begin in  
138 November 2023. All observations up to April 2025 were included. This cutoff was established because,  
139 starting in June 2025, the first results of version D of the RiverSP product are released, whose geometric  
140 prior corresponds to SWORD v17b, whereas version C relies on SWORD v17. These two versions exhibit  
141 some geometric differences in channel traces, which may introduce inconsistencies when combining  
142 products. For this reason, the analysis was restricted exclusively to version C up to April 2025. Version D  
143 data were not considered because sufficiently long and stable time series for Chilean basins are not yet  
144 available to support a meaningful evaluation, and this study focuses on an initial assessment based on  
145 the most stable release currently available, while the mission team continues evaluating the geometric  
146 updates introduced in Version D.

147 Only observations meeting the criteria  $wse\_u < 0.15$  and  $node\_q = 0$  or  $1$  were retained to ensure the  
148 required minimum quality.

149 The spatial definition of reaches and nodes is derived from SWORD v17, which contains simplified vector  
150 geometries of global river systems. The accuracy of this database is critical for correctly matching  
151 satellite observations to actual channel sections; therefore, its geometric validity was assessed as part of  
152 the analysis. For this purpose, multispectral Sentinel-2 imagery (Copernicus Programme) was used to  
153 visualize river traces at a 10-m resolution. These images enabled verification of the actual channel  
154 location and the detection of discrepancies between SWORD geometry and the observed river position,  
155 supporting the identification of misalignment or geometric displacement errors in specific reaches of the  
156 Biobío and its tributaries.

### 157 ***2.2. In situ data – DGA streamflow stations***

158 As a validation reference, data from streamflow gauging stations administered by the DGA were used.  
159 Stations were selected based on their location in rivers observed by SWOT and the availability of records  
160 that temporally overlapped with the acquisition dates of the L2\_HR\_RiverSP product.

161 Instantaneous discharge records were employed, as these are the only datasets that include water level  
162 (stage) estimates with a temporal resolution of 30 minutes. However, not all stations had recent data  
163 due to the common delay between measurement dates and public availability in DGA systems.  
164 Consequently, in several cases, the time series had to be truncated before 2025, although efforts were  
165 made to maximize the temporal overlap with SWOT observations.

166 The DGA interpolates some values to preserve the 30-minute resolution, but the interpolation method is  
167 not specified. In all detected cases, the interpolation did not exceed one day of gap, allowing these  
168 values to be included without significantly affecting the fine-scale temporal comparison with SWOT.

169 In total, nine streamflow stations were selected, distributed along the Biobío River and its main  
170 tributaries. This coverage spans a wide range of channel widths and geomorphological conditions,  
171 enabling evaluation of the SWOT product's performance across contrasting river environments.

### 172 ***2.3. Temporal matching and vertical reference adjustment.***

173 To compare satellite observations with in situ records, an hourly temporal matching was performed  
174 using the SWOT acquisition time as the reference. This procedure was necessary because, in several of  
175 the analyzed sites, SWOT provided more than one observation per day (due to different orbital passes  
176 affecting the same node or adjacent nodes), and this ensured that the intraday variability captured by  
177 SWOT was not lost. Only observations with coincident timestamps were retained, and unmatched cases  
178 were excluded without interpolation.

179 Each DGA station was associated with three SWOT nodes from the L2\_HR\_RiverSP product (version C),  
180 selected based on geographic proximity. Nodes were chosen strictly by horizontal proximity within the  
181 same river segment to ensure hydraulic consistency. When no nearby nodes with available data were  
182 present, reach-level observations corresponding to the station's location were used instead.

183 Because SWOT-derived elevations are referenced to the EGM2008 geoid, whereas DGA series report  
184 water levels relative to a local (unspecified) gauging datum, a vertical reference adjustment was applied.  
185 For this purpose, the mean difference between the overlapping portions of both series was computed  
186 and applied as an additive correction, thereby aligning the datasets within a common relative reference  
187 frame.

### 188 ***2.4. Quality filters and validation metrics***

189 To ensure the quality of the satellite data, the following filters were applied:

- 190 • Only nodes with quality values of `node_q` = 0 or 1 were retained, as these correspond to valid  
191 observations without critical warnings.
- 192 • Observations with `wse_u`  $\geq$  0.15 were excluded, since high uncertainty values indicate a low level of  
193 confidence in the water-surface elevation estimate.

194

195

196

197

198 The comparison between SWOT time series and in situ data was carried out using standard hydrological  
 199 metrics (Alvial Vásquez et al., 2020; Moriasi et al., 2015; López-Pozo et al., 2022), computed using the  
 200 mean of the three SWOT nodes associated with each station (or the corresponding reach when no  
 201 nodes were available). The metrics used were:

202

203 *Table 1. Statistics used to evaluate the consistency between SWOT and in situ data.*

| Statistic  | Formula   | Ranges                                   |
|--|---|--|
| <b>Standardized standard deviation (<math>\sigma_e</math>)</b> | $\sigma_e = 1 - \frac{\sqrt{\sum_{i=1}^n (Y_i - \bar{Y})^2}}{(X_i - \bar{X})^2}$  | $(-\infty, 1]$ ( $\approx 0$ ideal)      |
| <b>Normalized root mean square error (NRMSE)</b>               | $nrmse = \frac{\sqrt{\sum_{i=1}^n (X_i - Y_i)^2}}{\sigma_x}$  | $[0, \infty)$ (less is better)           |
| <b>Mean absolute error (MAE)</b>                               | $MAE = \frac{1}{n} \sum_{i=1}^n  X - Y $  | $[0, \infty)$ (less is better)           |
| <b>Pearson correlation coefficient (R)</b>                     | $\rho_{xy} = \frac{\sum_{i=1}^n (X_i - \bar{X})(Y_i - \bar{Y})}{\sqrt{\sum_{i=1}^n (X_i - \bar{X})^2} \sqrt{\sum_{i=1}^n (Y_i - \bar{Y})^2}}$ | $[-1, 1]$ ( $ r $ high = Good agreement) |
| <b>Nash–Sutcliffe model efficiency coefficient (NSE)</b>       | $nse = 1 - \frac{\sum_{i=1}^n (X_i - Y_i)^2}{\sum_{i=1}^n (X_i - \bar{X})^2}$   | $(-\infty, 1]$ (1 ideal)                 |
| <b>Willmott's index of agreement (d)</b>                       | $d = 1 - \frac{\sum_{i=1}^n (Y_i - X_i)^2}{\sum_{i=1}^n ( Y_i - \bar{X}  +  X_i - \bar{X} )^2}$   | $[0, 1]$ (1 ideal)                       |

Let  $X_i$  denote the in-situ water-level observations (DGA), used as the reference series, and  $Y_i$  the corresponding SWOT-derived water-surface elevations.

204

205 NSE < 0 indicates poorer performance than the mean, NRMSE provides a normalized error measure,  
 206 MAE reflects absolute deviations, and the Willmott index (d) quantifies relative agreement, with values  
 207 approaching 1 indicating strong consistency. These metrics allow assessing both the agreement in shape  
 208 and magnitude between the series, as well as the presence of systematic biases. In all cases, the  
 209 statistics were interpreted according to the ranges reported in the hydrological literature.

## 210 **2.5. Spatial analysis and geomorphological assessment**

211 To evaluate the spatial consistency of SWOT observations, the density and quality of the data were  
 212 examined along different reaches of the river. Patterns of data loss, dispersion, and coverage gaps were  
 213 investigated and linked to physical channel characteristics such as width, riparian vegetation, and  
 214 morphology. Offsets were identified visually when the SWOT centerline clearly deviated from the  
 215 observable water surface.

216 In some reaches with poor performance, a detailed inspection was carried out using Sentinel-2 imagery  
 217 and the channel geometry recorded in the SWORD database, with the aim of identifying possible  
 218 alignment errors, mislocated nodes, or “dark water” conditions that may hinder radar detection.

219 **2.6. Uncertainty analysis of the SWOT product**

220 In addition to the validation against in situ data, an independent evaluation of the uncertainty reported  
 221 by the L2\_HR\_RiverSP product (wse\_u) was conducted for all nodes within the Biobío River basin.

222 In the uncertainty analysis, all available nodes inside the basin boundary were considered, without  
 223 restricting the sample to those associated with gauging stations. The wse\_u < 0.15 filter was not applied,  
 224 in order to capture the full distribution of uncertainty in the product. However, the node quality  
 225 criterion was maintained, retaining only observations with node\_q = 0 or 1, thereby ensuring a minimum  
 226 level of geometric and instrumental reliability. Estimated channel widths for each node were also  
 227 incorporated, as SWOT uncertainty depends strongly on channel morphology, particularly in narrow,  
 228 sinuous, or densely vegetated rivers.

229 **3. Results**

230 **3.1. Statistical validation of SWOT observations**

231 The results obtained from the comparison between SWOT L2\_HR\_RiverSP satellite observations and in  
 232 situ records from the DGA are summarized in Table 2. Nine gauging stations distributed across different  
 233 reaches of the Biobío River basin were evaluated, using standard hydrological metrics to quantify the  
 234 agreement between both data sources.

235 *Table 2. Comparison of SWOT measurements with in situ observations.*

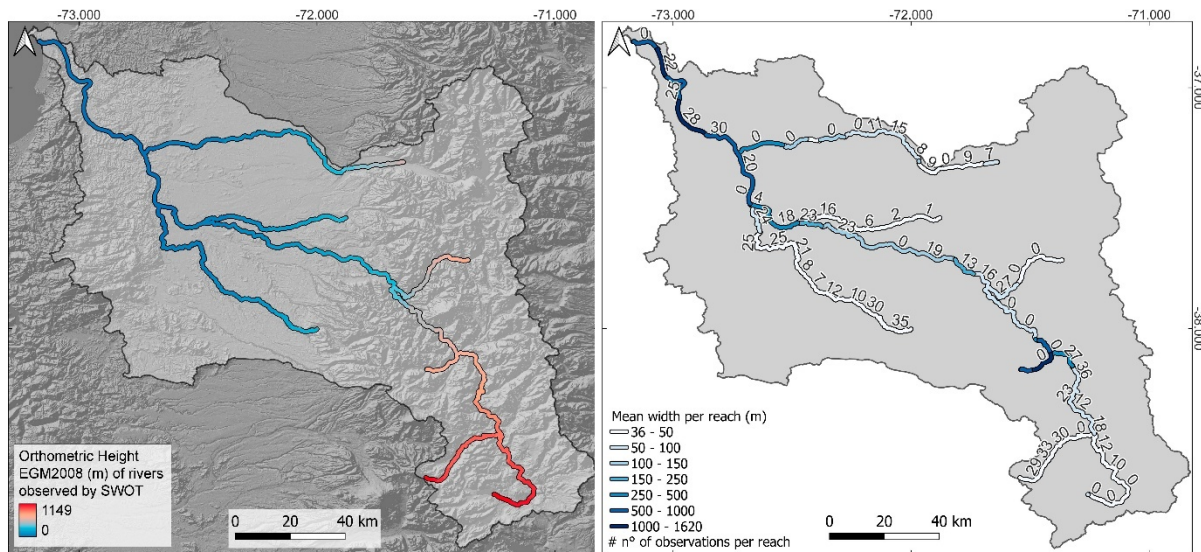
| Gauging Station                      | $\sigma_e$ | nRMSE | MAE  | R    | NSE    | d    | N° obsv | Start Date | Max width river (m) |
|--------------------------------------|------------|-------|------|------|--------|------|---------|------------|---------------------|
| Río Biobío Ante Junta Pangue         | -1.58      | 2.27  | 0.99 | 0.42 | -4.50  | 0.52 | 16      | 20-01-2024 | 42                  |
| Río Biobío en Coihue                 | -0.15      | 1.10  | 0.42 | 0.46 | -0.27  | 0.68 | 18      | 14-05-2025 | 270                 |
| Río Biobío en Desembocadura          | -0.12      | 0.28  | 0.11 | 0.97 | 0.92   | 0.98 | 27      | 10-12-2023 | 2389                |
| Río Biobío en Llanquén               | -0.48      | 1.46  | 0.79 | 0.34 | -1.18  | 0.60 | 61      | 29-11-2023 | 54                  |
| Río Biobío en la Culebra             | -4.59      | 4.83  | 0.60 | 0.61 | -24.45 | 0.38 | 12      | 09-12-2024 | 67                  |
| Río Duqueco en Cerrillos             | 0.71       | 1.24  | 1.19 | 0.19 | -0.63  | 0.40 | 20      | 12-04-2024 | 39                  |
| Río Duqueco en Villucura             | 0.25       | 0.69  | 0.22 | 0.71 | 0.51   | 0.81 | 25      | 29-11-2023 | 48                  |
| Río Laja en Tucapel 2                | -0.27      | 0.71  | 0.28 | 0.83 | 0.48   | 0.89 | 29      | 20-01-2024 | 67                  |
| Río Lonquimay Antes Junta Rio Biobío | 0.54       | 0.69  | 0.78 | 0.51 | 0.75   | 0.02 | 38      | 2023-12-09 | 36                  |

236

237 As shown in Table 2, there is a relationship between channel width and the performance of the satellite  
 238 product, although this relationship is not strictly linear. Good results were observed in some relatively  
 239 narrow reaches, whereas in other, even wider sections, the agreement was less optimal. This suggests  
 240 that local morphology and hydraulic complexity influence the performance of SWOT as much as the  
 241 effective river width.

242 In stations located in wider reaches, such as Biobío en Desembocadura (2,389 m) and Laja en Tucapel 2  
 243 (67 m), correlation coefficients were high ( $R \approx 0.97$  and  $R \approx 0.83$ , respectively), and relative errors  
 244 (NRMSE  $\approx 0.28$  and  $0.71$ ) remained below  $0.75$ . These values, together with positive NSE scores ( $\approx 0.92$   
 245 for Biobío en Desembocadura and  $\approx 0.48$  for Laja en Tucapel 2), indicate an acceptable representation of  
 246 hydrological dynamics by SWOT in these reaches.

247 In contrast, stations associated with narrow or geomorphologically complex rivers, such as Duqueco en  
 248 Cerrillos (39 m) and Biobío en La Culebra (67 m), showed negative NSE values and substantial dispersion  
 249 between the series (e.g., NRMSE  $\approx 1.24$  at Duqueco en Cerrillos and  $\approx 4.83$  at Biobío en La Culebra).  
 250 These results reflect the limited detection capacity of the satellite radar under such conditions, where  
 251 the signal is more sensitive to channel irregularities and to the partial loss of water pixels.



252

253 *Figure 2. (Left) Water surface elevation of rivers observed by SWOT. (Right) Average channel width of SWOT-measured reaches*  
 254 *and number of observations per reach.*

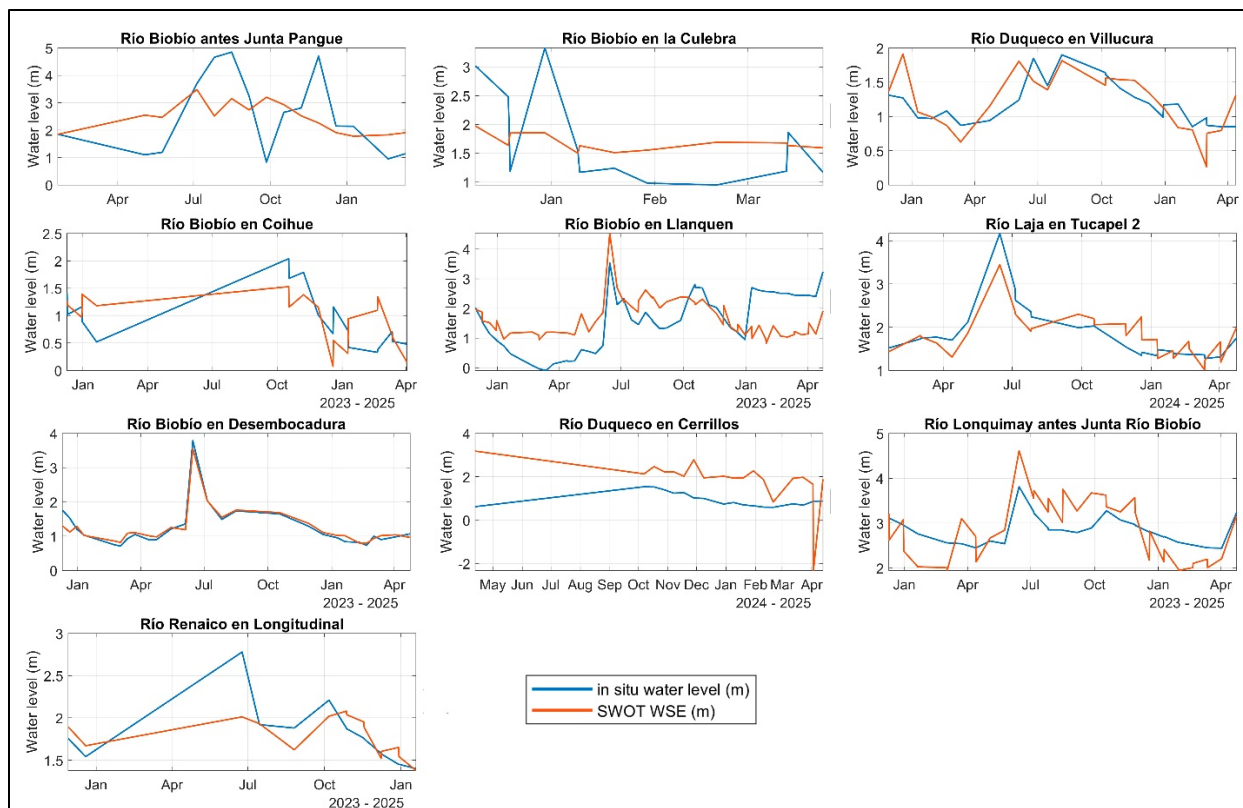


Figure 3. Time series at selected sites for the comparison between SWOT data and in situ water level measurements

255  
256

257 A particular case is the station Lonquimay Antes Junta Río Biobío, for which no temporally matching data  
 258 were available, neither at the node level, as shown in Figure 4, nor for the respective reach. In this  
 259 scenario, the three closest nodes of the Biobío River, located immediately downstream of the  
 260 confluence, were used as an approximation to evaluate the hydrological evolution at this point.  
 261 Although this comparison is not strictly correct, it provides a reasonable reference for the river  
 262 dynamics, considering that both rivers exhibit similar responses up to the confluence zone due to their  
 263 comparable morphologies and shared climatic conditions. Despite being different rivers, a high  
 264 correlation was obtained ( $R \approx 0.78$ ), which is a strong indication that the mission is able to capture  
 265 hydrological dynamics even in very narrow reaches (<50 m). This reach is characterized by its  
 266 narrowness and dense riparian vegetation, conditions that hinder satellite detection of the water  
 267 surface and may explain the reduced performance observed. Although the Biobío reach immediately  
 268 downstream of the confluence contains more SWOT observations, a direct hydrological comparison is  
 269 not possible due to the absence of gauging stations in that area.

270 Other reaches, such as Biobío en Coihue and Biobío Ante Junta Pangué, showed only partial  
 271 reproduction of the temporal signal, with moderate correlations ( $R \approx 0.46$  and  $0.42$ ), but negative NSE  
 272 values and substantial magnitude errors ( $\text{NRMSE} \approx 1.10$  and  $2.27$ ). These patterns are consistent with  
 273 the presence of river islands, riparian vegetation, or irregular channel geometries that are not  
 274 adequately represented in SWOT, which can introduce errors in the assignment of water surfaces and  
 275 reduce agreement between SWOT and in situ series.

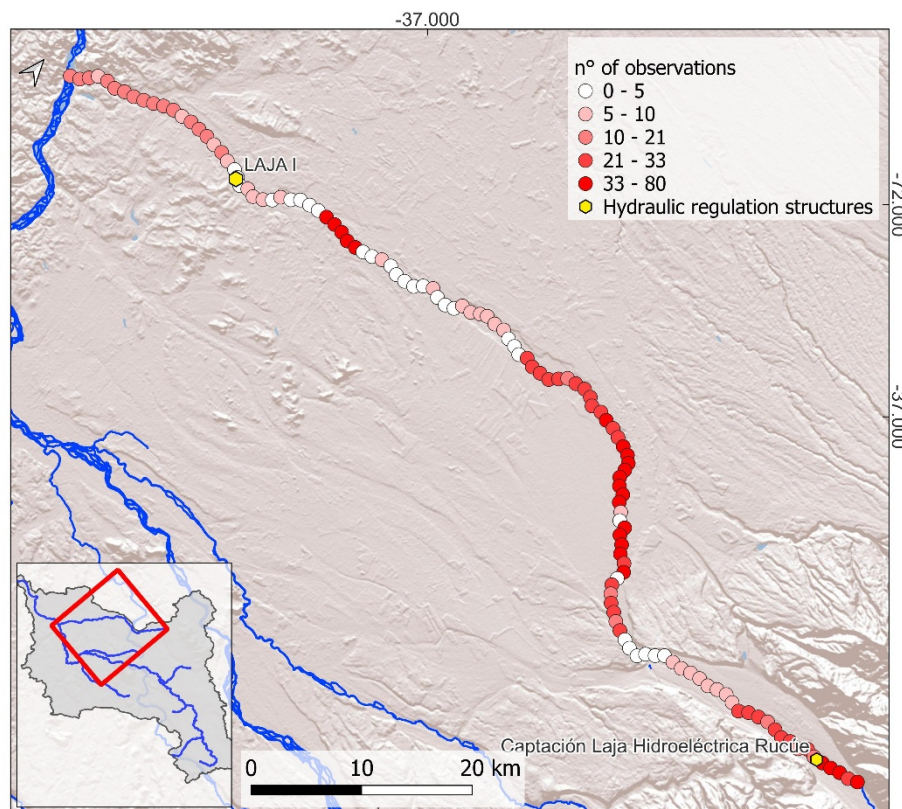
276 A reduction in the quality and consistency of observations was detected starting in May 2025, coinciding  
 277 with the transition of the SWOT product from version C to version D. This update introduced new height

278 calibrations and adjustments to reach geometries, which may have generated discontinuities in the time  
279 series at certain sites. These observations were not included in the calculation of the statistical metrics.

### 280 **3.2. Spatial variability in SWOT observation coverage and quality**

281 Beyond the metric differences between stations, a high degree of spatial variability was observed in the  
282 coverage and quality of satellite observations along the river channels. This heterogeneity appeared  
283 even within the same river, where adjacent reaches exhibit markedly different densities of valid  
284 observations, as illustrated in Figure 2.

285 For example, in the Laja River, certain narrow reaches contained a considerable number of observations  
286 with acceptable uncertainty, whereas other, wider downstream sections showed significantly lower  
287 coverage. Figure 4 highlights this abrupt alternation, indicating that the variability cannot be explained  
288 solely by channel width. In some areas, channel depth remains constant or even increases, suggesting  
289 the influence of additional factors such as water-surface roughness (“dark water”), reduced flow  
290 velocity, or riparian vegetation.



291  
292 *Figure 4. Number of SWOT node observations in the Laja River.*

293 In hydraulically regulated areas, such as the reach upstream of the LAJA I Hydroelectric Plant, channel  
294 widening was associated with a smoother water surface, which may reduce the radar backscatter  
295 detectable by SWOT. Similarly, at the confluence of the Lonquimay River with the Biobío, a higher  
296 number of SWOT observations is recorded in the Biobío, even though the Lonquimay exhibits  
297 comparable morphological conditions.

298 In addition, a general increase in the number of available observations was identified after the transition  
299 of the SWOT product from version C to version D, although no formal comparative analysis was  
300 performed. Many of the nodes with lower data density shown in Figure 4 do not account for the dates of  
301 this update, suggesting that the new geometric calibrations or filtering algorithms may have improved  
302 effective detection in certain fluvial contexts.

### 303 **3.3. Temporal variability**

304 In certain reaches with a sufficient number of observations, it was possible to examine the temporal  
305 evolution of water levels observed by SWOT in comparison with in situ measurements from the DGA.  
306 The best results were obtained at Biobío en Desembocadura and Laja en Tucapel 2, although temporal  
307 patterns could also be identified, albeit with lower quality, in stations such as Biobío en Llanquén and  
308 Duqueco en Villucura, where the time series exceeded 20 valid observations.

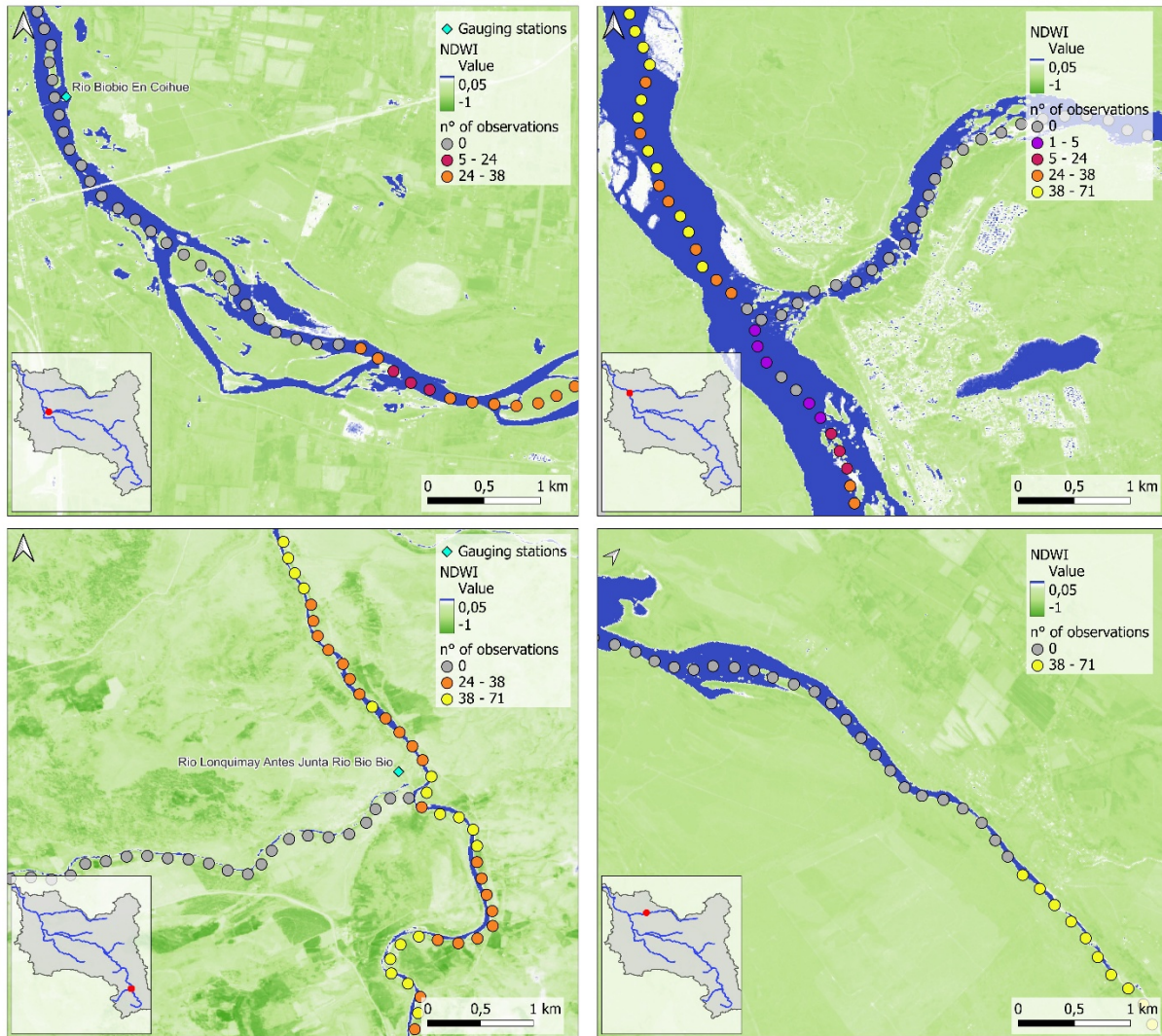
309 In the case of Biobío en Llanquén, the overall performance metrics were  $R = 0.34$ ,  $NSE = -1.18$ , and  
310  $NRMSE = 1.40$ . Nevertheless, periods of good visual agreement between both datasets were identified,  
311 particularly between June and October 2024, as shown in Figure 3.

312 For Río Biobío Ante Junta Pangué ( $R = 0.42$ ), SWOT partially reproduced the temporal shape of the  
313 signal, although with substantial magnitude errors. The limited number of available observations  
314 increases the statistical uncertainty of the resulting metrics.

315 Taken together, the analyzed stations showed appreciable temporal variability in the quality of the  
316 match between satellite observations and in situ records, as evidenced by differences in correlation  
317 levels and scatter throughout the time series.

### 318 **3.4. Geometric analysis and positioning errors (Sentinel-2)**

319 In addition to the validated stations, a geometric and quantitative assessment was conducted for river  
320 reaches without DGA coverage, using SWOT observations and Sentinel-2 optical products. The objective  
321 was to identify physical or geometric factors that could explain the low density or quality of satellite  
322 observations, as well as possible misalignments between the SWOT database and the actual position  
323 of the river channel.



324  
 325 *Figure 5. River positions captured by Sentinel-2 in 2015 and the corresponding SWORD Prior Database node locations. Río Biobío*  
 326 *en Coihue (upper left), Laja–Biobío confluence (upper right), Río Lonquimay Antes Junta Río Biobío (lower left) and*  
 327 *Laja River (lower right).*

328 In the lower section of the Laja River, an abrupt alternation was observed between reaches with more  
 329 than 30 detections per year (and over 60 detections for the full period of available records) and others  
 330 with fewer than 10 valid detections, even though the average channel width remains relatively constant  
 331 at around 30–60 m. This discontinuity is not associated with local hydrological variations but rather with  
 332 differences in georeferencing and geometric segmentation of reaches in the SWORD v17 database.

333 As can be seen in figure 5, at the confluence of the Laja and Biobío rivers, the number of valid  
 334 observations decreased by more than 68% over the final 29 km before the junction, despite channel  
 335 width increasing from 50–100 m to more than 200 m. Conversely, at the confluence of the Lonquimay  
 336 River with the Biobío, the number of SWOT observations in the Biobío is approximately ten times higher  
 337 than in the Lonquimay, even though both exhibit similar mean widths ( $\approx 45$  m) but different slopes  
 338 (0.15% for the Lonquimay and 0.38% for the Biobío at the confluence). These contrasts confirm the  
 339 influence of reach geometry and flow orientation on the radar’s detection capability.

340 Figure 5 illustrates these patterns and reveals localized geometric errors in the SWORD database,  
 341 particularly in the Lonquimay River, where satellite nodes show displacements of 10 to 100 m relative to  
 342 the actual river trace observed in Sentinel-2 imagery. These misalignments cause between 10% and 12%  
 343 of SWOT observations to be assigned to incorrect channel sections, reducing effective coverage and  
 344 distorting the reported mean water-surface elevations.

### 345 **3.5. Relationship between uncertainty and channel width**

346 The data showed a clear relationship between channel width and the uncertainty associated with water-  
 347 level estimation (*wse\_u*), as illustrated in the scatterplot in Figure 6. The narrowest rivers exhibited the  
 348 highest uncertainties and the greatest dispersion. In the <50 m class, *wse\_u* reached a mean of 0.222 m  
 349 with a high standard deviation (0.314 m) and maximum values exceeding 25 m, indicating the presence  
 350 of severe errors associated with narrow, sinuous, or vegetated geometries where PIXC processing tends  
 351 to degrade. This uncertainty decreases progressively across wider classes: 0.129 m of uncertainty in 50–  
 352 100 m wide rivers, 0.116 m of uncertainty in 100–250 m wide rivers, and 0.106 m of uncertainty in >250  
 353 m wide rivers, reflecting that SWOT operates with greater stability in wider channels. Nevertheless, even  
 354 in wide rivers, a significant number of outliers were observed (up to 5.03 m), demonstrating that the  
 355 signal is not entirely free of extreme noise, although its relative frequency is much lower.

356 *Table 3. Descriptive statistics of channel width and wse\_u uncertainty by width classes, with and without outliers.*

| Node measured river width (m) |       |        |        |        |        |        |        |          |
|-------------------------------|-------|--------|--------|--------|--------|--------|--------|----------|
| Width class                   | count | mean   | std    | min    | 25%    | 50%    | 75%    | max      |
| < 50 m                        | 24585 | 27.92  | 14.61  | 0.00   | 16.35  | 30.01  | 40.59  | 50.00    |
| 50–100 m                      | 25311 | 72.60  | 14.24  | 50.00  | 60.19  | 71.37  | 84.47  | 100.00   |
| 100–250 m                     | 27965 | 159.31 | 42.29  | 100.01 | 122.31 | 151.96 | 192.00 | 249.98   |
| > 250 m                       | 36635 | 750.64 | 654.70 | 250.01 | 380.76 | 598.33 | 885.72 | 39804.24 |

| Node wse u (m) |       |         |         |         |         |         |         |          |
|----------------|-------|---------|---------|---------|---------|---------|---------|----------|
| Width class    | count | mean    | std     | min     | 25%     | 50%     | 75%     | max      |
| < 50 m         | 24585 | 0.22243 | 0.31385 | 0.09001 | 0.11376 | 0.14121 | 0.21740 | 25.09399 |
| 50–100 m       | 25311 | 0.12853 | 0.07581 | 0.09004 | 0.10182 | 0.11034 | 0.13173 | 3.26356  |
| 100–250 m      | 27965 | 0.11630 | 0.08345 | 0.09001 | 0.09561 | 0.10071 | 0.11342 | 3.27203  |
| > 250 m        | 36635 | 0.10615 | 0.07211 | 0.09000 | 0.09188 | 0.09348 | 0.09886 | 5.03176  |

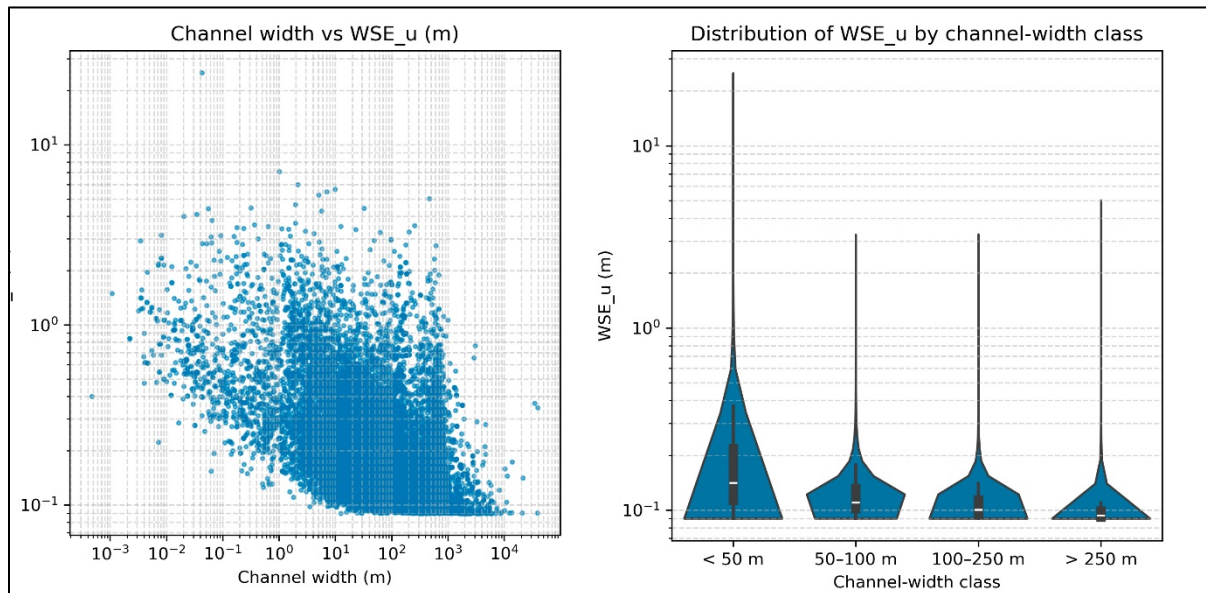
  

| Node measured river width (m) outliers removed |       |        |        |        |        |        |        |          |
|--|-------|--------|--------|--------|--------|--------|--------|----------|
| Width class                                    | count | mean   | std    | min    | 25%    | 50%    | 75%    | max      |
| < 50 m   | 22055 | 29.98  | 13.44  | 0.01   | 20.07  | 31.94  | 41.43  | 50.00    |
| 50–100 m                                       | 23159 | 72.96  | 14.22  | 50.00  | 60.58  | 71.99  | 84.84  | 100.00   |
| 100–250 m                                      | 25296 | 160.53 | 42.35  | 100.01 | 123.34 | 153.94 | 193.53 | 249.98   |
| > 250 m  | 31460 | 782.12 | 594.99 | 250.01 | 394.29 | 631.14 | 956.66 | 38948.39 |

| Node measured river width (m) outliers removed |       |         |         |         |         |         |         |         |
|--|-------|---------|---------|---------|---------|---------|---------|---------|
| Width class                                    | count | mean    | std     | min     | 25%     | 50%     | 75%     | max     |
| < 50 m   | 22055 | 0.15729 | 0.06154 | 0.09001 | 0.11202 | 0.13347 | 0.18316 | 0.37280 |
| 50–100 m                                       | 23159 | 0.11513 | 0.01895 | 0.09004 | 0.10124 | 0.10848 | 0.12331 | 0.17658 |
| 100–250 m                                      | 25296 | 0.10339 | 0.01090 | 0.09001 | 0.09530 | 0.09939 | 0.10792 | 0.14013 |
| > 250 m  | 31460 | 0.09434 | 0.00392 | 0.09000 | 0.09172 | 0.09292 | 0.09545 | 0.10933 |

357 After removing outliers using the IQR method, a more moderate characterization of the uncertainty  
 358 inherent to the SWOT product is obtained. Mean wse\_u values decreased systematically across all width  
 359 classes, but the most notable change occurs in narrow rivers: in the <50 m class, the mean decreases  
 360 from 0.222 m to 0.157 m, and the standard deviation drops from 0.314 m to only 0.062 m, indicating  
 361 that much of the extreme error corresponds to anomalous cases rather than the typical performance of  
 362 the algorithm. In wide rivers (>250 m), the uncertainty excluding outliers is even more constrained, with  
 363 a mean of 0.094 m and a standard deviation of only 0.0039 m, confirming an extremely stable signal  
 364 when channel geometry favors detection.



365  
 366 *Figure 6. Scatterplot illustrating the variation of WSE\_u uncertainty as a function of channel width: global dispersion (left) and*  
 367 *violin plots by width class (right).*

368 Figure 6 shows the relationship between channel width and wse\_u uncertainty across all available  
 369 observations. In the scatterplot, the dispersion of wse\_u is considerably higher in narrow rivers,  
 370 particularly in the <50 m class, where values exhibit a wide range and a clear concentration of high-  
 371 uncertainty points. As channel width increases, the point cloud progressively narrows, indicating a  
 372 general reduction in variability, although high values persist across all classes. This pattern is also  
 373 reflected in the violin plots, where the distributions are wider in channels narrower than 50 m and  
 374 become more compact in the broader width classes, while still retaining the presence of outliers. Taken  
 375 together, both visualizations show that uncertainty decreases overall as channel width increases, but  
 376 extreme variability is not completely eliminated from the dataset.

377 **4. Discussion**

378 The performance of the SWOT L2\_HR\_RiverSP product in the Biobío River basin shows clear spatial  
 379 variability controlled by channel width, morphology, and geometric accuracy of the SWOT database. In  
 380 wide and morphologically stable reaches, SWOT achieved its best results, with correlations above 0.80  
 381 and relatively low normalized errors. For example, the Biobío en Desembocadura, a reach exceeding two  
 382 kilometers in width, reached  $R = 0.92$  with an NRMSE of 0.28, while the Laja en Tucapel 2, although  
 383 considerably narrower, still achieved  $R = 0.83$  with an NRMSE below 0.75. These results are consistent

384 with global findings that document stronger SWOT performance in wide, regular channels (Andreadis et  
385 al., 2025; Du et al., 2023; Zhao et al., 2025).

386 Performance declined sharply in narrow or geomorphologically complex rivers. Stations such as  
387 Duqueco en Cerrillos and Biobío en La Culebra, both with widths well below 100 m, showed negative  
388 NSE values and normalized errors exceeding 1, confirming the known limitations of SWOT in channels  
389 narrower than 100 m (Andreadis et al., 2025; Gehring et al., 2023). Although moderate correlations  
390 were sometimes observed, such as  $R = 0.61$  at La Culebra, the magnitude of the errors indicates a strong  
391 sensitivity to sinuosity, vegetation, and confined topography.

392 Intermediate performance appeared in reaches like Biobío en Coihue and Biobío en Llanquén, where  
393 correlations ranged between 0.30 and 0.50 and errors remained moderate to high. At Llanquén,  
394 agreement improved notably during a specific seasonal window between June and October 2024,  
395 suggesting that hydrodynamic conditions, such as discharge variability and surface roughness, can affect  
396 radar detectability, in line with observations in other basins (Desrochers et al., 2021).

397 Significant heterogeneity was also observed in the number of valid SWOT detections, particularly in the  
398 Laja River, where some reaches accumulated over 60 valid observations while adjacent sections had  
399 fewer than 10, despite similar widths. Reductions in detection density of more than 60 percent were  
400 also observed near the Laja-Biobío confluence. These discontinuities are consistent with “dark water”  
401 effects associated with regulated flows, which reduce radar backscatter (Lobry et al., 2019).

402 Geometric inconsistencies in the SWORD v17 database played a critical role in several reaches. In the  
403 Lonquimay River, Sentinel 2 imagery indicated displacements on the order of tens of meters between  
404 actual river traces and SWORD node positions. These misalignments can shift SWOT detections entirely  
405 outside the true channel, explaining between 10 and 12 percent of erroneous observations in affected  
406 segments, consistent with similar issues reported elsewhere (Altenau et al., 2021; Larnier et al., 2024).

407 The uncertainty analysis further supports these findings. Narrow rivers typically exhibited mean  
408 uncertainties near 0.22 m, with large dispersion and occasional extreme values reaching several meters,  
409 while wide rivers showed considerably lower and more stable uncertainties, generally near 0.10 m. After  
410 removing statistical outliers, uncertainties in narrow channels dropped substantially but remained  
411 higher than in wider ones, indicating intrinsic limitations related to width, vegetation, and local  
412 geomorphology.

413 Temporal consistency also showed signs of degradation after the product transition from version C to  
414 version D in mid 2025, likely due to changes in geometric priors. These observations were excluded from  
415 the core performance statistics.

416 Overall, the results confirm that SWOT has significant potential to complement hydrological monitoring  
417 in Chile, especially in basins with limited in situ data. However, its performance depends strongly on  
418 channel width, morphology, hydraulic regulation, and the geometric reliability of SWORD. The Biobío  
419 basin, with its combination of wide lowland rivers and narrow Andean tributaries, provides an effective  
420 testbed for understanding these dynamics. As in other regions, operational use of SWOT in Chile will  
421 require local validation, geometric correction of river traces, and complementary analyses using lower  
422 level products such as PIXC (Desrochers et al., 2021; Dhote et al., 2025; Signorile et al., 2024).

423

## 424 5. Conclusions

425 Our results demonstrate that the performance of the SWOT L2\_HR\_RiverSP product in the Biobío basin  
426 is controlled primarily by channel width, local morphology, and the geometric accuracy of SWORD. Wide  
427 river sections, exceeding 200 m, consistently produced high correlations and moderate errors, whereas  
428 narrow or sinuous reaches yielded negative NSE values and large dispersion, confirming a strong  
429 morphological constraint on SWOT detectability. Geometric inconsistencies in SWORD and the reduced  
430 stability observed after the transition to version D further reveal that channel misalignment and evolving  
431 priors remain critical sources of uncertainty in complex fluvial environments.

432 These findings indicate that, although SWOT represents a transformative opportunity for hydrological  
433 monitoring in countries like Chile where in situ networks are sparse and unevenly distributed, its  
434 operational use in steep, narrow, or heavily regulated rivers requires rigorous local validation. The  
435 systematic influence of width, vegetation, sinuosity, and hydraulic alteration highlights the need for  
436 integrating SWORD refinement and lower-level products such as PIXC to diagnose and mitigate  
437 observation failures.

438 This study provides the first basin-scale evaluation of SWOT performance in Andean river systems and  
439 establishes a quantitative foundation for future high resolution altimetry-based SWOT hydrological  
440 monitoring in Chile. Expanding the analysis across additional climatic and hydrological conditions, and  
441 testing the robustness of new product versions, will be essential to ensure reliable, long-term use of  
442 SWOT in data-scarce and geomorphologically complex regions.

## 443 6. Acknowledgments

444 Mauricio Sepúlveda is supported by Fondecyt-ANID Project 1220869 and ANID-Chile through Centro de  
445 Modelamiento Matemático, Universidad de Chile (FB210005).

446 Fernando Campos is supported by ANID scholarship ANID-PCHA/Doctorado Nacional 21242229.

447 Generative AI was used to assist in the translation of this manuscript from Spanish to English.

## 448 7. References

449 Altenau, E. H., Durand, M., Smith, L. C., et al. (2021). The Surface Water and Ocean Topography (SWOT)  
450 Mission River Database (SWORD): A global river network for satellite data products. *Water Resources*  
451 *Research*, 57(7), e2021WR030054. <https://doi.org/10.1029/2021WR030054>

452 Alvial Vásquez, F.-J., Abarca-del-Río, R., & Ávila, A. I. (2020). High-Resolution Precipitation Gridded  
453 Dataset on the South-Central Zone (34° S–41° S) of Chile. *Frontiers in Earth Science*, 8.  
454 <https://doi.org/10.3389/feart.2020.519975>

455 Amaral, F. R. d., Pellarin, T., Trung, T. N., Tu, T. A., & Gratiot, N. (2024). Enhancing discharge estimation  
456 from SWOT satellite data in a tropical tidal river environment. *PLOS Water*, 3(2), e0000226.  
457 <https://doi.org/10.1371/journal.pwat.0000226>

458 Andreadis, K. M., Coss, S. P., Durand, M., Gleason, C. J., Simmons, T. T., Tebaldi, N., et al. (2025). A first  
459 look at river discharge estimation from SWOT satellite observations. *Geophysical Research Letters*, 52,  
460 e2024GL114185. <https://doi.org/10.1029/2024GL114185>

461 Andreoli, A., Mao, L., Iroumé, A., Arumí, J. L., Nardini, A., Pizarro, R., Caamaño, D., Meier, C., & Link, O.  
462 (2012). The need for a hydromorphological approach to Chilean river management. *Revista Chilena de*  
463 *Historia Natural*, 85, 339–343. <http://dx.doi.org/10.4067/S0716-078X2012000300008>

464 Elizabeth H. Altenau, Tamlin M. Pavelsky, Michael T. Durand, Xiao Yang, Renato P. d. M. Frasson, & Liam  
465 Bendezu. (2025). SWOT River Database (SWORD) (Versión v17) [Data set]. Zenodo.  
466 <https://doi.org/10.5281/zenodo.14727521>

467 Biancamaria, S., Lettenmaier, D. P., & Pavelsky, T. M. (2016). The SWOT Mission and Its Capabilities for  
468 Land Hydrology. *Surveys in Geophysics*, 37(2), 307–337. <https://doi.org/10.1007/s10712-015-9346-y>

469 Desrochers, N. M., Trudel, M., Biancamaria, S., Siles, G., Desroches, D., Carbonne, D., & Leconte, R.  
470 (2021). Effects of Aquatic and Emergent Riparian Vegetation on SWOT Mission Capability in Detecting  
471 Surface Water Extent. *IEEE Journal of Selected Topics in Applied Earth Observations and Remote*  
472 *Sensing*, 14, 12467-12478. <https://doi.org/10.1109/JSTARS.2021.3128133>

473 Dhote, P., et al. (2025). SWOT mission with wide-swath altimetry: Observations and insights into India's  
474 inland waterbodies. *Journal of the Indian Society of Remote Sensing*, 53, 2367–2376.  
475 <https://doi.org/10.1007/s12524-025-02234-8>

476 Dirección General de Aguas (DGA). (2012). Estudio hidrogeológico cuenca del río Biobío: Informe final y  
477 planos (Tomo I). Aquaterra Ingenieros Ltda., División de Estudios y Planificación, Ministerio de Obras  
478 Públicas, Gobierno de Chile.

479 Du, J., Zhang, S., Li, Y., Wang, J., Chen, X., & Hong, Y. (2023). Accurate discharge estimation based on  
480 river widths of SWOT and constrained at-many-stations hydraulic geometry. *Remote Sensing*, 15(6),  
481 1672. <https://doi.org/10.3390/rs15061672>

482 Dirección General de Aguas (DGA). (2012). Estudio hidrogeológico cuenca del río Biobío: Informe final y  
483 planos (Tomo I). Aquaterra Ingenieros Ltda., División de Estudios y Planificación, Ministerio de Obras  
484 Públicas, Gobierno de Chile. [https://bibliotecadigital.ciren.cl/items/4873abb9-7277-4aa0-96e6-](https://bibliotecadigital.ciren.cl/items/4873abb9-7277-4aa0-96e6-b705553a7e11)  
485 [b705553a7e11](https://bibliotecadigital.ciren.cl/items/4873abb9-7277-4aa0-96e6-b705553a7e11)

486 Figueroa, R., Parra, O., & Díaz, M. (2020). La cuenca hidrográfica del río Biobío. En Centro EULA-Chile  
487 (Ed.), *EULA-Chile: Evolución y perspectivas a 30 años de su creación* (pp. 91-138). Universidad de  
488 Concepción <https://bibliotecadigital.ciren.cl/items/b28cde3c-6ef6-4030-aff0-dbe5c015c32e>

489 Fustos, I., Abarca-del-Río, R., Artal, O., Alvial, F., & Sepúlveda, H. H. (2022). Impact on discharge  
490 modelling using different spatial and temporal resolution scenarios in South of Chile. *Journal of South*  
491 *American Earth Sciences*, 115, 103727. <https://doi.org/https://doi.org/10.1016/j.jsames.2022.103727>

492 Gehring, J., Gleason, C. J., Durand, M., Smith, L. C., Pavelsky, T. M., & Andreadis, K. M. (2023). Assessing  
493 the potential for the SWOT mission to monitor narrow rivers and streams. *Frontiers in Earth Science*, 11,  
494 1201711. <https://doi.org/10.3389/feart.2023.1201711>

495 Hrachowitz, M., et al. (2013). A decade of Predictions in Ungauged Basins (PUB)—A review. *Hydrological*  
496 *Sciences Journal*, 58(6), 1198–1255. <https://doi.org/10.1080/02626667.2013.803183>

497 JPL. (2025). SWOT Product Description Document: Level 2 KaRIn High Rate River Single Pass Vector  
498 (L2\_HR\_RiverSP) Data Product (JPL D-56413, Rev. C). Jet Propulsion Laboratory.

499 Krasovskaia, I., & Gottschalk, L. (2002). River flow regimes in a changing climate. *Hydrological Sciences*  
500 *Journal*, 47(4), 597–609. <https://doi.org/10.1080/02626660209492962>

501 Larnier, K., et al. (2024). Estimating channel parameters and discharge at river-network scale using  
502 hydrological–hydraulic models, SWOT and multi-satellite data. *Water Resources Research*, 60(5),  
503 e2024WR038455. <https://doi.org/10.1029/2024WR038455>

504 Ledauphin, T., Garambois, P.-A., Larnier, K., Azzoni, M., Emery, C., Picot, N., Amzil, S., Fjørtoft, R.,  
505 Maxant, J., & Yésou, H. (2025). Assessing SWOT's Hydraulic Visibility on the Rhine: Precision Flow Lines  
506 and Slope-Based Flood Wave Propagation Signatures. *Earth and Space Science*, 12(7), e2025EA004309.  
507 <https://doi.org/https://doi.org/10.1029/2025EA004309>

508 Lobry, S., Denis, L., Williams, B., Fjørtoft, R., & Tupin, F. (2019). Water Detection in SWOT HR Images  
509 Based on Multiple Markov Random Fields. *IEEE Journal of Selected Topics in Applied Earth Observations*  
510 *and Remote Sensing*, 12(11), 4315–4326. <https://doi.org/10.1109/JSTARS.2019.2948788>

511 Lopez-Pozo, F., Abarca-del-Rio, R., & Lara, L. E. (2022). ADTC-InSAR: A tropospheric correction database  
512 for Andean volcanoes. *Scientific Data*, 9(1), 526. <https://doi.org/10.1038/s41597-022-01630-w>

513 Malmqvist, B., & Rundle, S. (2002). Threats to the running water ecosystems of the world.  
514 *Environmental Conservation*, 29(2), 134–153. <https://doi.org/10.1017/S0376892902000097>

515 Mesa Nacional del Agua. (2022). Informe final. Ministerio de Obras Públicas, Gobierno de Chile.  
516 <https://pre-dga.mop.gob.cl/informe-final-mesa-nacional-del-agua>

517 Moreira, D., Papa, F., Fassoni-Andrade, A., Fleischmann, A., Wongchuig, S., Paiva, R., et al. (2025).  
518 Widespread and exceptional reduction in river water levels across the Amazon Basin during the 2023  
519 extreme drought revealed by satellite altimetry and SWOT. *Geophysical Research Letters*, 52,  
520 e2025GL116180. <https://doi.org/10.1029/2025GL116180>

521 Moriasi, D. N., Gitau, M. W., Pai, N., & Daggupati, P. (2015). Hydrologic and water quality models:  
522 Performance measures and evaluation criteria. *Transactions of the ASABE*, 58(6), 1763–1785.

523 Nicolás Vásquez, J. C., Gómez, T., Mendoza, P. A., Lagos, M., Boisier, J. P., & Álvarez-Garretón, C. (2021).  
524 *Water Resources of Chile (Vol. 8)*. Springer. <https://doi.org/10.1007/978-3-030-56901-3>

525 Organisation for Economic Co-operation and Development (OECD). (2024). *OECD Environmental*  
526 *Performance Reviews: Chile 2024 (Chapter 2, “Water management and policies”)*. OECD Publishing.  
527 <https://doi.org/10.1787/5bc65d36-en>

528 Paiva, R. C. D., Moreira, D., & Papa, F. (2022). SWOT for South America: Cal/Val and applications to  
529 South American river systems. Technical Report. SWOT Science Team, Jet Propulsion Laboratory (NASA).

530 Patidar, G., Indu, J., & Karmakar, S. (2025). Performance assessment of Surface Water and Ocean  
531 Topography (SWOT) mission for WSE measurement across India. *Geophysical Research Letters*, 52,  
532 e2025GL115804. <https://doi.org/10.1029/2025GL115804>

533 Petry, I., Fan, F. M., & Wood, A. W. (2025). Observed streamflow data shows El Niño–Southern  
534 Oscillation increases likelihood of extreme events in South America. *Communications Earth &*  
535 *Environment*, 6(1), 699. <https://doi.org/10.1038/s43247-025-02714-2>

536 Poff, N., Allan, J. D., Bain, M., Karr, J., Prestegard, K., Richter, B., Sparks, R., & Stromberg, J. (1997). The  
537 Natural Flow Regime: A Paradigm for River Conservation and Restoration. *Bioscience*, 47.

538 Rojas, Octavio, Mardones, María, Arumí, José Luis, & Aguayo, Mauricio. (2014). Una revisión de  
539 inundaciones fluviales en Chile, período 1574-2012: causas, recurrencia y efectos geográficos. *Revista de*  
540 *geografía Norte Grande*, (57), 177-192. <https://dx.doi.org/10.4067/S0718-34022014000100012>

541 Signorile, M., et al. (2024). Riparian vegetation surveys for roughness estimation. *Journal of Hydrology*  
542 *and Environment Research*, 68(4), 223–240. <https://doi.org/10.1016/j.ecoleng.2024.107414>

543 Stehr, A., et al. (2019). Recursos hídricos en Chile: Impactos y adaptación al cambio climático. Informe  
544 de la Mesa del Agua. <https://bibliotecadigital.ciren.cl/handle/20.500.13082/32329>

545 Surface Water and Ocean Topography (SWOT). (2024). SWOT Level 2 River Single-Pass Vector Data  
546 Product (Version C). PO.DAAC, CA, USA. <https://doi.org/10.5067/SWOT-RIVERSP-2.0>

547 Theia. (2025, March 26). SWOT: Understanding our rivers, lakes and flood-plains. [https://www.theia-](https://www.theia-land.fr/en/blog/swot-understanding-our-rivers-lakes-and-floodplains/)  
548 [land.fr/en/blog/swot-understanding-our-rivers-lakes-and-floodplains/](https://www.theia-land.fr/en/blog/swot-understanding-our-rivers-lakes-and-floodplains/)

549 Vásquez, N., Cepeda, J., Gómez, T., Mendoza, P. A., Lagos, M., Boisier, J. P., Álvarez-Garretón, C., &  
550 Vargas, X. (2021). Catchment-scale natural water balance in Chile. In B. Fernández & J. Gironás (Eds.),  
551 *Water Resources of Chile* (pp. 189–208). Springer. [https://doi.org/10.1007/978-3-030-56901-3\\_9](https://doi.org/10.1007/978-3-030-56901-3_9)

552 Wade, J., David, C. H., Collins, E. L., Denbina, M., Cerbelaud, A., Tom, M., Reager, J. T., Frasson, R. P. M.,  
553 Famiglietti, J. S., Lee, T., & Gierach, M. M. (2025). Intrinsic spatial scales of river stores and fluxes and  
554 their relative contributions to the global water cycle. *Geophysical Research Letters*, 52(4),  
555 e2024GL113052. <https://doi.org/10.1029/2024GL113052>

556 Wang, J., Sheng, Y., Allen, G., & Crétaux, J.-F. (2020). Integrating reservoirs into SWOT's global surface  
557 water storage and discharge monitoring (Technical report). SWOT Science Team, Jet Propulsion  
558 Laboratory (NASA). Retrieved from  
559 [https://swot.jpl.nasa.gov/system/documents/files/4172\\_SWOT\\_\\_Summary\\_Wang\\_Sheng\\_Allen\\_Cretaux\\_](https://swot.jpl.nasa.gov/system/documents/files/4172_SWOT__Summary_Wang_Sheng_Allen_Cretaux_06262020.pdf)  
560 [x\\_06262020.pdf](https://swot.jpl.nasa.gov/system/documents/files/4172_SWOT__Summary_Wang_Sheng_Allen_Cretaux_06262020.pdf)

561 Yao, J., Xu, N., Wang, M., Liu, T., Lu, H., Cao, Y., ... Xu, H. (2025). SWOT satellite for global hydrological  
562 applications: Accuracy assessment and insights into surface water dynamics. *International Journal of*  
563 *Digital Earth*, 18(1). <https://doi.org/10.1080/17538947.2025.2472924>

564 Yoon, Y., Durand, M., Rodríguez, E., Alsdorf, D., Moller, D., & Smith, L. C. (2015). Estimating flood  
565 discharges in reservoir-regulated river basins by integrating synthetic SWOT satellite observations and  
566 hydrologic modeling. *Hydrology and Earth System Sciences*, 19(3), 1261–1275.  
567 [https://doi.org/10.1061/\(ASCE\)HE.1943-5584.0001320](https://doi.org/10.1061/(ASCE)HE.1943-5584.0001320)

568 Zeiringer, B., Seliger, C., Greimel, F., & Schmutz, S. (2018). River hydrology, flow alteration, and  
569 environmental flow. In *Riverine Ecosystem Management* (pp. 67–89). [https://doi.org/10.1007/978-3-](https://doi.org/10.1007/978-3-319-73250-3_4)  
570 [319-73250-3\\_4](https://doi.org/10.1007/978-3-319-73250-3_4)

571 Zhao, Y., Fu, J., Pang, Z., Jiang, W., Zhang, P., & Qi, Z. (2025). Validation of inland water surface elevation  
572 from SWOT satellite products: A case study in the Yangtze River. *Remote Sensing*, 17(8), 1330.  
573 <https://doi.org/10.3390/rs17081330>

# Centro de Investigación en Ingeniería Matemática (CI<sup>2</sup>MA)

## PRE-PUBLICACIONES 2025 - 2026

- 2025-23 EIDER ALDANA, RICARDO OYARZÚA, JESÚS VELLOJÍN: *Numerical analysis of a three-field formulation for a reverse osmosis model*
- 2025-24 JULIO ARACENA, FLORIAN BRIDOUX, MAXIMILIEN GADOULEAU, PIERRE GUILLON, KEVIN PERROT, ADRIEN RICHARD, GUILLAUME THEYSSIER: *On the Dynamics of Bounded-Degree Automata Networks*
- 2025-25 DANIEL CAJAS GUIJARRO, JOHN CAJAS GUIJARRO: *Resonant and non-resonant double Hopf bifurcation in a 4D Goodwin model with wage inequality*
- 2025-26 ALONSO J. BUSTOS, SERGIO CAUCAO: *A Banach space mixed formulation for the unsteady Brinkman problem with spatially varying porosity*
- 2025-27 JULIO ARACENA, KATERIN DE LA HOZ, ALEXIS POINDRON, LILIAN SALINAS: *An exploratory approach to the compatibility and inference of unate functions*
- 2025-28 JESSIKA CAMAÑO, SERGIO CAUCAO, CRISTIAN INZUNZA: *A five-field mixed formulation for the fully dynamic Biot–Brinkman model*
- 2025-29 JUAN BARAJAS-CALONGE, MAURICIO SEPÚLVEDA, NICOLÁS TORRES, LUIS M. VILLADA: *Dynamically consistent finite volume scheme for a bimonomeric simplified model with inflammation processes for Alzheimer’s disease*
- 2026-01 ALONSO J. BUSTOS, GABRIEL N. GATICA, RICARDO RUIZ-BAIER, BENJAMÍN N. VENEGAS: *A perturbed threefold saddle-point formulation yielding new mixed finite element methods for poroelasticity with reduced symmetry*
- 2026-02 JORGE AGUAYO, RODOLFO ARAYA: *A Nitsche-type finite element method for the linear elasticity equation with discontinuity jumps*
- 2026-03 SERGIO CAUCAO, GABRIEL N. GATICA, ADRIAN SUAREZ, IVAN YOTOV: *A skew-symmetry-based mixed formulation for an Oseen-type Kelvin–Voigt–Brinkman–Forchheimer model*
- 2026-04 AKBAR DAVOODI, DIANA PIGUET, HANKA RADA, NICOLÁS SANHUEZA-MATAMALA: *The asymptotic version of the Erdős–Sós conjecture and beyond*
- 2026-05 RODRIGO ABARCA DEL RIO, FERNANDO CAMPOS, CRISTÓBAL CARO-RAMÍREZ, JEAN FRANÇOIS CRETAUX, DANIEL MOREIRA, ALFREDO RIBEIRO NETO, JONAS FELIPE SANTOS DE SOUZA, MAURICIO SEPÚLVEDA: *First insights into the performance of the SWOT Level 2 River Single-Pass Vector Data Product in rivers with complex morphology: application to the Bío-Bío River basin, Chile*

Para obtener copias de las Pre-Publicaciones, escribir o llamar a: DIRECTOR, CENTRO DE INVESTIGACIÓN EN INGENIERÍA MATEMÁTICA, UNIVERSIDAD DE CONCEPCIÓN, CASILLA 160-C, CONCEPCIÓN, CHILE, TEL.: 41-2661324, o bien, visitar la página web del centro: <http://www.ci2ma.udec.cl>



**CENTRO DE INVESTIGACIÓN EN  
INGENIERÍA MATEMÁTICA (CI<sup>2</sup>MA)  
Universidad de Concepción**



Casilla 160-C, Concepción, Chile  
Tel.: 56-41-2661324/2661554/2661316  
<http://www.ci2ma.udec.cl>

